

INDENTATION OF AN S_2 FLOATING ICE SHEET IN THE BRITTLE RANGE

by

B. Michel and D. Blanchet*

(Laboratoire de Mécanique des Glaces, Département de Génie Civil, Université Laval, Ste-Foy, Québec G1K 7P4, Canada)

ABSTRACT

The problem of a floating ice sheet hitting a structure with a vertical face appears to be a simple one but, in fact, has only been solved for a limited number of cases. Research work on this question usually reports on an indentation coefficient which relates the average pressure on the indenter to the uniaxial crushing strength of the ice. Very few tests have been made in the brittle range of ice failure. In this particular area of study, this paper reports on 27 tests that were conducted in a cold-room water basin where controlled S_2 floating ice sheets were produced with a surface area of 4 x 4 m, three sides being fully restrained and the other, freely floating, being submitted to the impact of the moving indenter. All tests were carried out at computed indentation rates varying from 0.017 to 0.34 s⁻¹. In this range this ice would normally be considered to act as a brittle material. The thickness of the ice sheets varied from 1.2 to 9.0 cm and the indenter width from 5 cm to 1 m. Overall, the aspect ratio relating these two parameters could be varied from 0.5 to 83.

Results have shown that for aspect ratios <5, there was an important oscillatory effect which caused the formation of plastified triangles in front of the indenter, increasing its resistance as it would under ductile conditions. Because of this plastification, an extrusion effect appeared in front of the indenter as the broken ice crystals were blown up and down in front of the fast-moving indenter. The theory of plasticity which gives an indentation coefficient of 2.97 seems to apply in this case. Another mode of failure which occurred with aspect ratios <5 was cleavage in the plane of the ice sheet which also gives a higher indentation coefficient for S_2 ice, but of the same order of magnitude as previously.

For intermediate values of the aspect ratio, between 5 and 20, the theory of elasticity used by Michel (1978) seems to apply well. Shear cracks are first formed on both sides of the square indenter and control the maximum pressure when they propagate inside forming big triangles in front of it.

Finally, for aspect ratios ~>20, buckling of the ice occurs, either after or at the same time as the formation of wedges, together with a reduction in the indentation coefficient to a value close to that given by the theory of buckling of a truncated 45° wedge with a hinged edge.

1. STATEMENT OF THE PROBLEM

Research on the impact of ice on structures has increased considerably in the last ten years and numerous articles have been published on the subject. Most of this research has been, however, theoretical, and there has been little experimental data to support the results.

Two completely different modes of failure were found experimentally when an indenter penetrates into an ice sheet (Michel and Toussaint 1977). In the ductile mode, at low speeds, microcracks are formed in individual ice grains which multiply to form a plastified zone in front of the indenter, progressing in a regular manner and producing a continuous load variation. In the brittle mode, at high speeds, macrocracks are formed in front of the indenter extending away from it and giving a highly fluctuating load. In the transition zone both mechanisms are observed.

In many ways the ductile behaviour can be represented by the theory of elastic-plastic failure. But this does not appear to be the case for brittle fracture which combines the very complex processes of macro- and microcracking as well as buckling of the floating ice. This is the least known of the problems related to the impact of ice on a vertical-faced structure though it is a most important one for engineering applications. This question was the object of this experimental study.

In general, all research on this question is related to the earlier work of Korzhavin (1962) who suggested the following empirical relationship:

$$p = C_j m k \sigma, \quad (1)$$

where

$$F = 2b h p. \quad (2)$$

In these equations, 2b is indenter width, C_j indentation coefficient, F total ice force (load), h ice thickness, m form coefficient (1 for a rectangular indenter), k contact coefficient (1 for full contact), p effective ice pressure, and σ uniaxial crushing strength of ice obtained for similar ice on small samples.

Although Equation (1) is widely accepted with the relevant m and k values, the discussions centre around the adequate values to use for C_j and the choice of representative values for σ . In Korzhavin's original work the indentation coefficient and the ice

*Now with Dome Petroleum Ltd., PO Box 200 Calgary, Alberta T2P 2H8, Canada.

strength were grouped in what he called the indentation strength σ_j :

$$\sigma_j = C_j \sigma \quad (3)$$

He then proposed that this indentation strength was decreased with increasing velocities and suggested a relationship in order to compute this value for different velocities. However, many other authors found that the so-called indentation strength was an increasing function of velocity (e.g. Saeki and others 1978). Michel and Toussaint (1977) found experimentally that in the ductile range the indentation strength followed exactly the dependence of the uniaxial crushing strength of ice on strain-rate (or velocity). This function is shown on Figure 1.

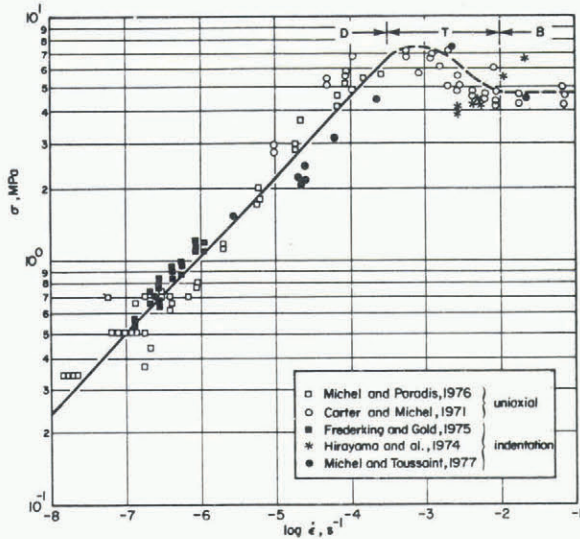


Fig.1. General curve for uniaxial crushing and indentation of S_2 ice at -10°C (σ is strength and $\dot{\epsilon}$ is strain-rate). A coefficient of 3 has been used to reduce the indentation data in the ductile zone (D) and transition zone (T), and 1.57 in the brittle zone (B). Refer to Michel (1978) for description of data.

Little is known, however, about the value that should be given to C_j in the transition and brittle range, which is of a broader practical interest.

The more widely held view is that C_j is a function of $2b/h$. The value of C_j is usually taken to start at ~ 3 for very narrow indenters (i.e. $2b/h$ small) and to attain a value of 1 for large values of $2b/h$. This was originally suggested by Afanas'yev (1972). Recent theoretical analyses used a limit plastic analysis with the upper and lower bound theorems (Croasdale and others 1977, Ralston 1978). For a narrow indenter, Croasdale and others showed that the problem reduces to that of a classical Prandtl indenter with $C_j = 2.57$ when using a failure criterion of the Tresca type. For large values of $2b/h$ the ice would fail by forming a wedge across the ice thickness as was originally proposed by Tryde (1973). The applicability of a plastic analysis to ice behaviour in the brittle range may be challenged.

In the ductile range, Michel and Toussaint (1977) carried out laboratory experiments on plates of highly anisotropic S_2 ice. These plates, 81×81 cm, were held vertically in a press and were indented with flat indenters. They found that C_j was independent of $2b/h$ with the exception of very narrow indenters where the size of the ice grains became relatively important. The value of the indentation factor was then found to be close to 3 and this could be explained with the Hill theory of indentation in a perfect plastic material, using the Von Mises failure

criterion. The computed value of C_j is then 2.97. They also showed that the experimentally observed dependence of the indentation factor on the width of the structure is caused only by the strain-rate effect on the yield strength of ice, in compression. This occurred only at low indentation speeds.

In the brittle range for the same S_2 ice, Michel (1978) suggested $C_j = 1.57$, obtained from the perfectly elastic solution with the Tresca failure criterion. Such a value was proposed previously for all cases of ice impact by Kheysin (1961). This coefficient is also independent of $2b/h$ with this theory.

It is possible that the approach giving a value of $C_j = 1$ may be rationalized if the completely different failure modes for isotropic ice and columnar S_2 ice under conditions of plane stresses are taken into account, as explained in a recent paper by Michel (1981) and shown in Figure 2. Isotropic ice can easily fail by formation of wedges in the vertical plane (first proposed by Tryde (1973)), but S_2 ice must first fail by indentation in the plane of the ice cover before it can shear across its thickness.

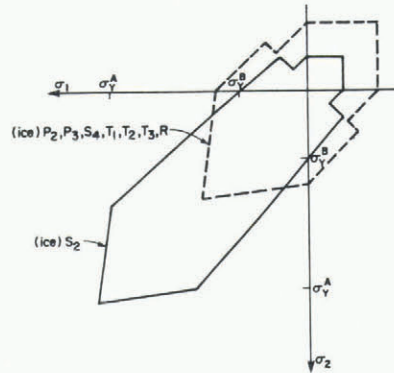


Fig.2. Failure envelope for both columnar (full line) and granular ice (dashed line) under conditions of plane stresses. Ice types are indicated and σ_1 and σ_2 are positive in the compression zone. σ_A is the strength to fail the ice across the plane and σ_B is the strength to fail the ice across the plane and σ_C is the strength to fail the ice across the plane and σ_D is the strength to fail the ice across the plane (Michel 1981).

In this paper we present new experimental data on the failure of floating ice sheets of S_2 ice made in a laboratory tank, under a fast-moving vertical-faced indenter.

2. LABORATORY RESULTS

Twenty-seven tests were carried out in a cold-room water basin with a surface area of 4×4 m as shown in Figure 3.

2.1. The experimental set-up

The basin itself was built within a steel frame acting as a loading press to which the ice sheet was attached. Its maximum capacity was 110 kN for an indenter 1 m wide and an ice thickness of 2.5 cm. The water depth was 60 cm. The ice sheet was produced by seeding, growing and, then, selective melting of the top layer in order to obtain uniform S_2 ice without the random crystal orientation normally present on the top of natural S_2 ice. Crystal sizes were, on average, 2 mm. One side of the ice sheet was free-floating and directly aligned with the initial position of the indenter. The hydraulic ram had a diameter of 6.35 cm and a stroke of 1.83 m so that more than one significant load event could be obtained. Three cells were used to measure the loading force in two different manners. A potentiometer measured the distances and an accelerometer the accelerations. The ram was operated with a maximum speed of 6.8 cm s^{-1} which gave computed indentation rates varying from 0.017 to 0.34 s^{-1} . In this

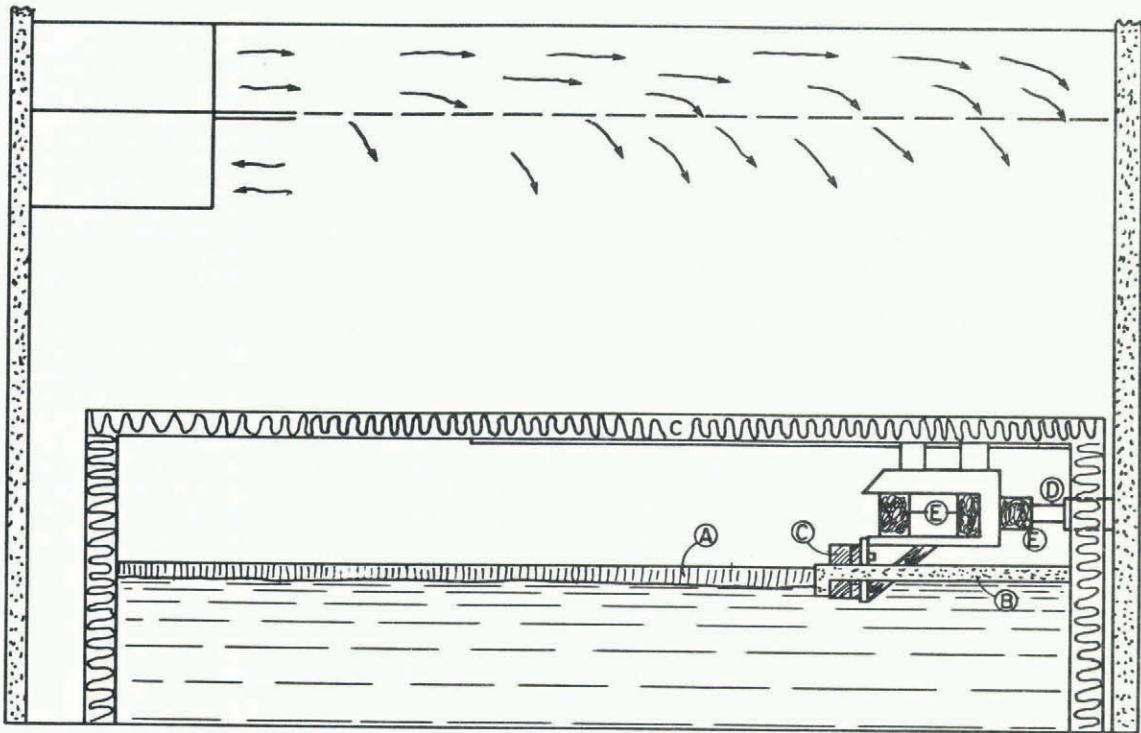


Fig.3. Sketch of the indentation basin with the ice sheet in the cold room. A is the ice sheet, B the plastic foam to form the free edge, C the loading edge, D the piston, and E the load cells.

range the ice can normally be considered to act as a brittle material.

All measurements were recorded on a HP-1000 data acquisition system with an interval of 0.01 s between recordings.

2.2. Program of testing

All tests were carried out at an air temperature of 0°C to ensure a uniform strength within the ice sheet. Only S_2 ice was tested so that major parameters to be varied were those of the aspect ratio $2b/h$ of the indenter. Since both b and h could be combined in different ways, tests were made with constant values of $2b/h$ whilst varying b and h . The description of the 27 tests is given in Table I.

2.3. Results of tests

The results for all tests conducted are given in Table II. The characteristic length of ice for buckling analyses is λ ; all other parameters have been defined previously. The uniaxial crushing strength was taken as 2.2 MPa from previous tests for this ice in the brittle range. Values for m and k in Equation (1) were both taken as 1 in the computations. These results are all shown on graphical form in Figure 4 giving C_i as a function of $2b/h$.

3. INTERPRETATION OF RESULTS

For all tests the horizontal force was recorded and the broken ice sheet was reconstituted afterwards to determine the fracture lines. A film was also taken in each case to analyze and record the manner in which the ice failed.

The aspect ratio $2b/h$ was varied from 0.5 to 83 and four different modes of failure were observed. Although each mode was found in ranges of $2b/h$ which overlapped with one another, it is easier for description and understanding to separate each mode of failure within a specified range of $2b/h$ whilst keeping in mind this overlapping effect.

3.1. Failure by cleavage, $2b/h < 1$

For very small indenters, as in test 1, the ice may fail by cleavage across its thickness. The terms of peeling or spalling may also describe this process.

Usually, however, this type of failure is combined with extrusion.

In this case radial cracks first appeared at the corners of the indenter making wedge angles from 5 to 35° with the direction of motion. The ice was peeled in a dish-like fashion over the top third and the bottom third of the ice thickness.

A typical recording for test 1 is shown in Figure 6. The maximum force was obtained when the initial cleavage process occurred and the value for C_i was found to be 2.4.

The value of C_i may thus be the experimental value of failure of columnar S_2 ice across its thickness by cleavage. This has been found experimentally to be between 2 and 3 in the top range of ductile failure (Frederking and Gold 1975). After the first two peaks there was a large reduction in load as the peeling continued in the remaining section. This was also observed in tests that were previously carried out (Michel and Toussaint 1977).

3.2. Failure by plastification in a triangle and extrusion, $2b/h < 5$

This is the general mode of failure observed for small indenters, as in tests 2, 14, 15, 16a, 17, 18, 20 and 24. In these tests a triangle was first formed in front of the indenter by cracks making, on each side, angles from 15 to 30° with the direction of motion. Simultaneously, a tensile crack appeared at the vertex of the triangle in the direction of motion, as shown in Figure 5. The ice then plastified due to microcracking of the individual crystals within the triangle. This plastification was assisted by the loading system whose speed decreased throughout loading of the frame but increased as the load dropped. Finally, the plastified ice was blown up and down by extrusion in a thin layer just in front of the moving indenter and the process repeated itself once the indenter came again in contact with the remaining intact ice sheet.

A typical recording for test 2 is shown in Figure 7. The peak force was obtained during the extrusion process and appeared relatively constant from peak to peak for these tests. The maximum loads corresponded

TABLE I. SUMMARY OF ALL INDENTATION TESTS MADE IN S₂ ICE, θ = 0°C

Test	h (cm)	2b (cm)	2b/h	Velocity of indenter (cm s ⁻¹)	Indentation rate $\dot{\epsilon} = V/4b$ (s ⁻¹)	Diameter of grains (mm)
1	5.0	5	1.0	6.6	0.33	2.2
2	3.5	5	1.43	6.8	0.34	2.1
3	4.0	20	5.0	6.6	0.0825	2.5
4	3.0	20	6.67	6.6	0.0825	2.2
5	2.7	30	11.1	6.7	0.056	1.8
6	2.8	40	14.3	6.6	0.0413	2.1
7	1.8	60	33.3	6.8	0.0283	-
8	2.6	60	23.1	6.8	0.0283	2.2
9	3.2	60	18.8	6.7	0.0279	1.9
10	1.2	60	50.0	6.7	0.0279	3.5
11	2.5	100	40.0	6.8	0.017	1.9
12	1.5	100	66.7	6.7	0.0168	-
13	1.2	100	83.3	6.7	0.0168	1.9
14	3.6	6	1.67	6.8	0.283	2.2
15	2.2	6	2.73	6.6	0.275	2.0
16a	5.0	12	2.40	6.7	0.14	2.5
16b	4.2	12	2.86	6.8	0.142	2.3
17	5.0	5	1.0	6.8	0.33	2.4
18	7.2	5	0.69	6.8	0.34	2.7
19	5.2	15	2.88	6.7	0.112	2.4
20	9.0	5	0.56	6.6	0.33	2.9
23	2.2	60	27.3	6.7	0.028	2.0
24	2.0	10	5.0	6.8	0.17	2.1
26	2.1	20	9.52	6.8	0.085	2.0
27	2.0	40	20	6.7	0.042	1.9

to C_i varying between a wide range from 2.0 to 3.3. In this case, the value of C_i can probably be related to most theories of the ductile behaviour of ice (Croasdale and others 1977, Michel and Toussaint 1977, Ralston 1978) that give an indentation coefficient close to 3.

3.3. Shear failure, 5 < 2b/h < 20

The series for intermediate size and large indenters was characterized by macrocracking of the

ice sheet and can be represented by tests 4, 5, 11 and 26. In these tests, radial cracks originated initially from the corners of the indenter making angles from 0 to 30° with the direction of motion. These cracks propagated either outside to form wedges in the ice sheet or inside to form large broken triangles in front of the indenter. A major peak was recorded when these first cracks formed a triangle. At the beginning of each test there might be some

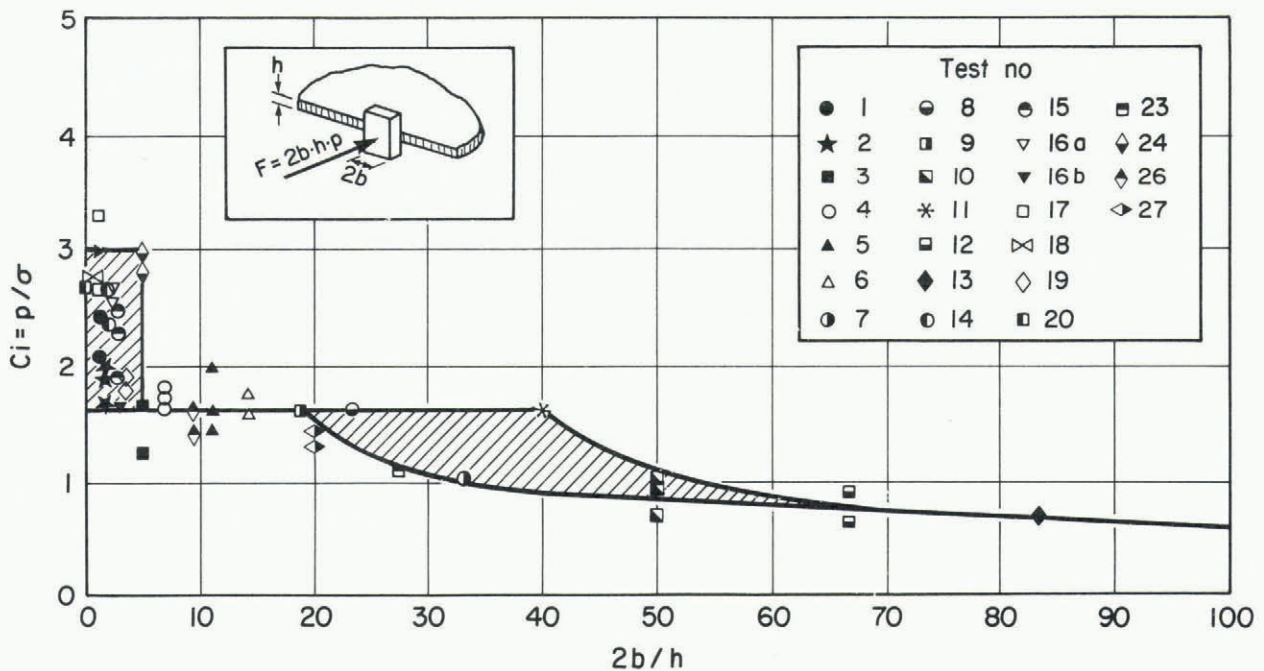


Fig.4. General curve of results of the tests giving C_i as function of 2b/h. The crossed areas show unstable zones.

ice extrusion just in front of the indenter but without noticeable plastification.

There was a drop in load immediately following the first crack formation. In one case of wedge formation, the first peak showed a higher intensity than the second one, which was caused by buckling of the wedge. This is shown in Figure 5. It then took a relatively long time until the indenter moved again

TABLE II. RESULTS OF TESTS GIVING PEAK LOADS AND COMPUTED INDENTATION COEFFICIENTS

Test	2b/h	F (kN)	Indentation pressure (MPa)	λ	$C_i (= P/\sigma, \text{ where } \sigma = 2.2 \text{ MPa})$
1	1.0	11.97	4.788	1.749	2.18
		13.42	5.367		2.44
2	1.43	6.33	3.617	1.338	1.64
		7.22	4.126		1.88
		7.77	4.44		2.02
3	5.0	13.83	1.729	1.479	0.78
		22.06	3.757		1.25
		28.43	3.554		1.62
4	6.67	15.91	2.653	1.192	1.21
		22.67	3.778		1.72
		21.76	3.627		1.67
		24.08	4.013		1.82
5	11.11	35.08	4.330	1.102	1.97
		27.71	3.421		1.56
		25.84	3.190		1.45
6	14.30	19.34	1.727	1.132	0.79
		43.13	3.851		1.75
		38.39	3.428		1.56
7	33.30	24.98	2.313	0.813	1.05
		14.16	1.311		0.60
8	23.10	55.73	3.512	1.071	1.60
		30.04	1.926		0.88
9	18.80	67.95	3.539	1.251	1.61
		36.19	1.885		0.86
10	50.0	11.07	1.538	0.600	0.70
		15.62	2.170		0.99
		16.13	2.240		1.02
11	40.0	87.94	3.518	1.04	1.60
12	66.7	21.54	1.436	0.709	0.65
		29.46	1.964		0.89
13	83.3	17.86	1.488	0.600	0.68
		17.93	1.494		0.68
14	1.67	11.37	5.264	1.367	2.39
		11.53	5.338		2.43
		12.75	5.903		2.68
15	2.73	5.47	4.144	0.945	1.88
		6.59	4.942		2.25
		7.31	5.538		2.52
16a	2.40	31.68	5.28	1.749	2.36
		35.88	5.98		2.68
		34.19	5.698		2.56
16b	2.86	18.09	3.59	1.534	1.61
		17.27	3.42		1.53
		17.89	3.55		1.59

TABLE II (continued)

Test	2b/h	F (kN)	Indentation pressure (MPa)	λ	$C_i (= P/\sigma, \text{ where } \sigma = 2.2 \text{ MPa})$
17	1.0	15.10	6.04	1.749	2.71
		14.78	5.91		2.65
		18.53	7.41		3.32
18	0.69	22.72	6.31	2.299	2.83
19	2.88	32.53	4.17	1.801	1.87
		28.55	3.66		1.64
		31.28	4.01		1.79
20	0.56	27.36	6.08	2.718	2.73
		26.78	5.95		2.67
23	27.3	32.08	2.43	0.945	1.10
24	5.0	13.01	6.51	0.880	2.95
		12.35	6.18		2.81
		12.52	6.26		2.85
		12.30	6.15		2.80
26	9.52	14.08	3.35	0.913	1.53
		12.63	3.02		1.37
		14.69	3.50		1.59
27	20	25.00	3.13	0.880	1.42
		22.35	2.80		1.27
		19.18	2.40		1.09

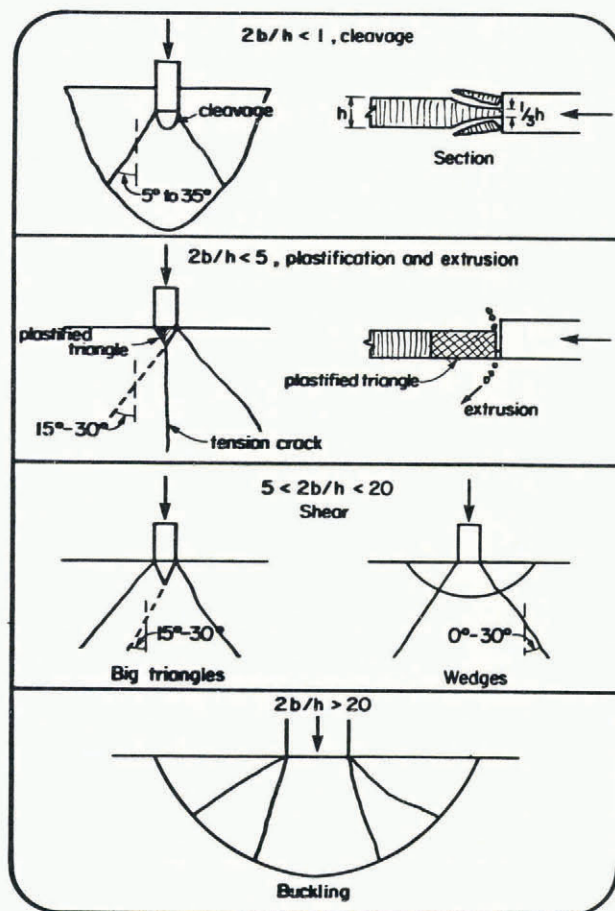


Fig.5. Sketches showing the different mechanisms of failure of the S_2 ice sheet in the brittle range for various values of $2b/h$.

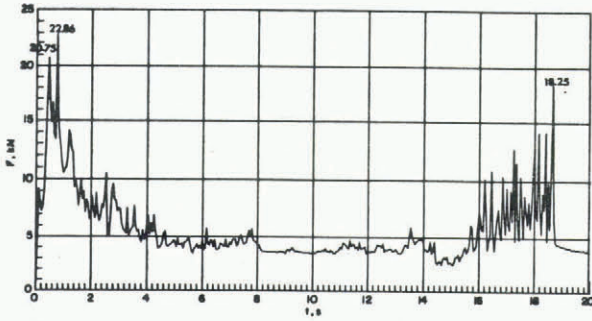


Fig. 6. Recording of loads for an ice sheet failing by cleavage (test 1).

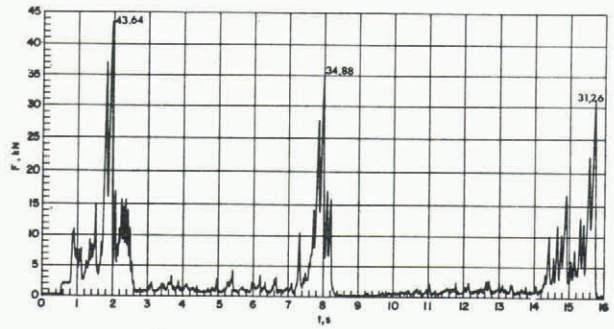


Fig. 9. Recording of loads for an ice sheet failing by shear with the formation of large triangles (test 8).

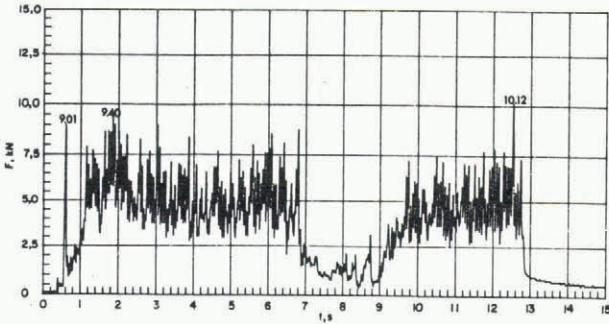


Fig. 7. Recording of loads for an ice sheet failing by formation of plastified triangles and extrusion (test 2).

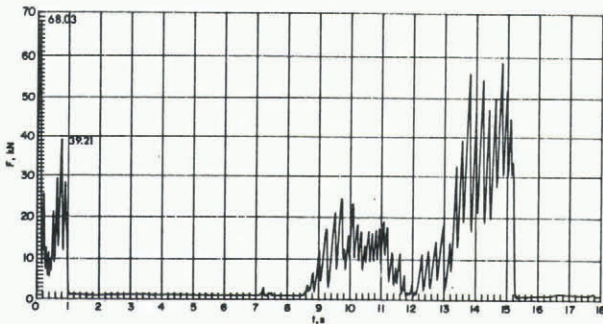


Fig. 8. Recording of loads for an ice sheet failing by shear with wedge formation and secondary buckling (test 5).

of motion, compared with zero for the elasticity theory, and slightly increases the computed value for C_j .

3.4. Buckling of the ice sheet, $2b/h \rightarrow 20$

Partial buckling was observed for tests 3, 6, 8, 9, 12 and 23 and general buckling in tests 7, 10, 25, and 27. In general, radial cracks first formed from the corners and were followed by buckling with little interruption in the increasing load. There was also some frontal extrusion occurring at the beginning of loading. The maximum load was given by buckling. A typical pattern of cracking after buckling is shown in Figure 5. It shows the radial and circumferential cracks. General buckling was not preceded by the formation of radial cracks, but all processes occurred simultaneously.

Figure 10 shows the successive buckling loads as the indenter moved into large broken ice pieces towards the intact sheet.

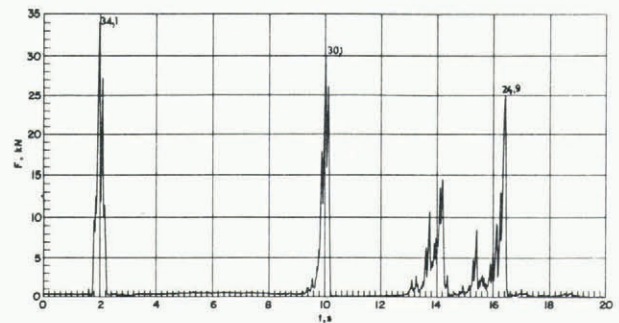


Fig. 10. Recording of loads for an ice sheet failing by successive buckling of wedges (test 27).

to the intact ice sheet and started building up the load again. When the ice buckled, circumferential cracks were formed in the ice.

When a large triangle was produced in front of the indenter, it was then pushed over the remaining ice sheet with a smaller force by the indenter. Load build-up started again from the renewed contact with the intact ice. A typical recording is shown on Figure 8 for test 8, when a wedge formed followed by buckling, or in Figure 9 for test 5, when a triangle was formed instead.

We believe that in all the tests in which triangles were formed the major event was the formation of the shear cracks at the corner of the indenter. When wedges were formed, shear was the controlling factor in only one case. From pure elasticity theory (Kheysin 1961, Michel 1978) C_j should then be 1.57 with the Tresca failure criterion. Measurements for all these tests gave C_j values varying from 1.53 to 1.97. We think that this small increase is caused by lateral friction on the ice by the indenter which prevents the ice from moving laterally. This produces shear cracks at angles up to 30° with the direction

Values of C_j for these tests fall in a range from 0.68 to 1.40. This is an important reduction compared with values for shear failure. In this interpretation, account has been taken of existing theories on buckling as shown in Figure 11. The dashed line is the curve given by Sodhi and Hamza (1978) and Nevel (1980) for the general buckling load of a semi-infinite sheet by a square-edged indenter with a free edge. The equation for this curve is:

$$\frac{F_{cr}}{\gamma \ell^3} = \frac{2b}{\ell} + \frac{3.32}{1+(b/2\ell)} \quad (4)$$

where F_{cr} is the buckling load, γ is the specific weight of water, and ℓ is the characteristic length given by:

$$\ell = \sqrt[4]{\frac{E h^3}{12(1-\nu^2)\gamma}} \quad (5)$$

Here, ν is Poisson's ratio and E is Young's modulus.

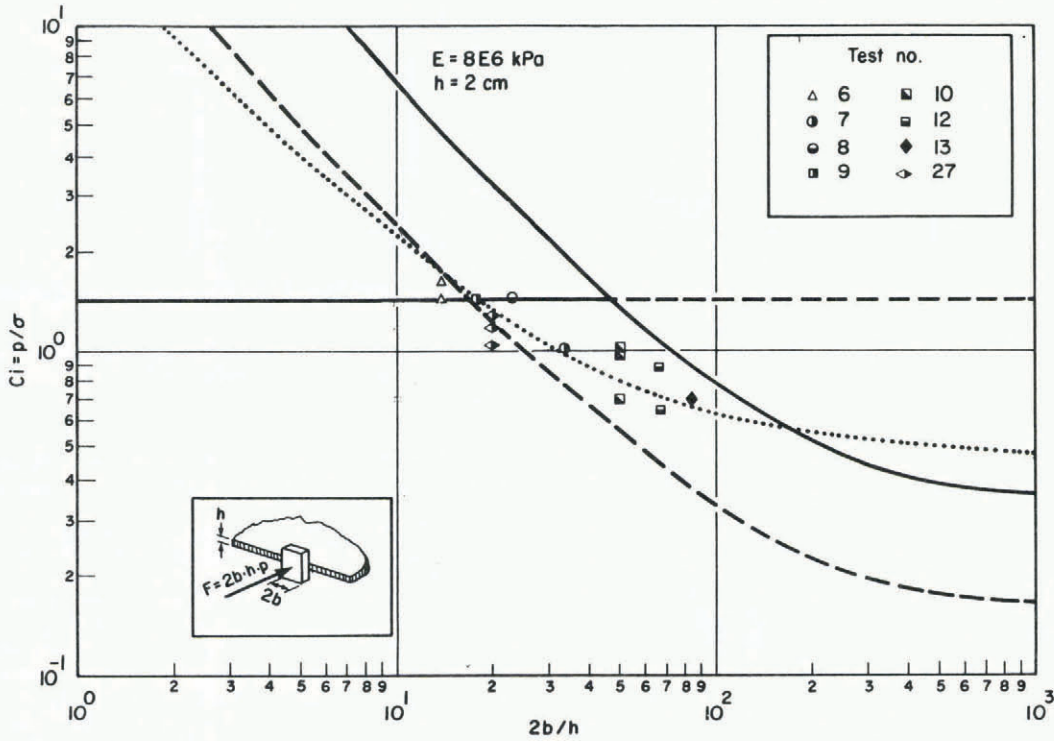


Fig.11. Data results for buckling. Three theoretical curves are shown, the dashed line for a free edge (Sodhi and Hamza 1978), the full line for a hinged edge (Elhadi and Dhatt 1981), and the dotted line for a hinged 45° wedge (Kerr 1978, 1981).

The upper full-line curve was obtained by Elhadi and Dhatt (1981) in a finite-element study for general buckling with a frictionless square-edged indenter with the ice hinged at the edge of the indenter. There is little doubt that this condition should be more representative than the condition of a free edge. In fact, the experimental data always show higher values than those from the curve given for a free edge, but they are still about 20% lower than the values given by the upper curve for a hinged edge. The dotted curve is the equation given by Kerr (1978, 1982) for partial buckling of a truncated wedge having a central angle ϕ and a loading width of $2b$. The equation in the case of a hinged end is:

$$\frac{F_{Cr}}{\gamma \ell^3} = 2.63 \left(\frac{2b}{\ell} + 2.08 \tan \frac{\phi}{2} \right). \quad (6)$$

The dotted curve in this equation was computed for an ice thickness of 2 cm and a central angle of 45°. It seems to represent most of the results well and intersects the shear failure line for $2b/h = 16$. This transition value depends obviously on ℓ and is different for various ice thicknesses and characteristics. For thicker ice it moves to higher values of $2b/h$ and, in fact, the condition for general buckling becomes more critical.

4. CONCLUSIONS

It is surprising to observe that for such a simple phenomenon as indentation of a uniform sheet of S_2 ice by a fast-moving square-edged indenter, four different failure mechanisms occur, depending on the aspect ratio, and only in the range of indentation rates in which ice would normally be considered to act as a brittle material. In the ductile range another completely different failure mode has been

observed previously when microcracking activity alone controlled the process of ice deformation.

S_2 ice is a non-isotropic type of ice which fails differently when loaded in the plane of the ice sheet than as opposed to it perpendicularly. If isotropic T_1 ice (snow ice) had been tested, the failure modes would have been different again, as neither cleavage nor in-plane plastic flow around the indenter could occur. The ice would then have failed by shear across the thickness of the ice sheet giving a much lower value of C_i , closer to 1 as proposed initially by Tryde (1973) for large indenters.

Even natural columnar ice would behave in a different manner because of the random orientation in space of the c-axis in the top centimetres of the ice sheet. For an observer the top ice would then shear to the top but the bottom ice would fail in the plane of the ice sheet. Taking into account the extremely important effect of temperature on the crushing strength of ice, it is not surprising that ice has always been one of the most difficult materials to study and analyze even under simple mechanical loading conditions.

In summary, for practical purposes S_2 would be more difficult to fail than other types of ice and would give values of C_i of the order of 3 for narrow structures with $2b/h < 5$, under quick loading conditions. It would also produce $C_i = 3$ for low loading rates for all structure widths, under ductile conditions (Michel and Toussaint 1977, Reinicke 1980). In the brittle range, it will give values of C_i around 1.8 for structures of intermediate size with $2b/h > 5$, and a much reduced value of C_i that could be computed for buckling conditions, with higher $2b/h$, depending on the thickness of the ice sheet.

ACKNOWLEDGEMENT

Support for this study was provided by the Natural Science and Engineering Research Council of Canada.

REFERENCES

- Afanas'yev V P 1972 Davleniye l'da na vertikal'nyye pregrady. *Transportnoye Stroitel'stvo* 3: 47-48 [English translation: Ice pressure on vertical structures. Canada. National Research Council. Technical Translation 1708, 1973]
- Carter D, Michel B 1971 Lois et mécanismes de l'apparente fracture fragile de la glace de rivière et de lac. Université Laval. Faculté des Sciences. Département de Génie Civil. Section Mécanique des Glaces. Rapport S-22
- Croasdale K R, Morgenstern N R, Nuttall J B 1977 Indentation tests to investigate ice pressures on vertical piers. *Journal of Glaciology* 19(81): 301-312
- Elhadi S M, Dhatt G S 1981 Instabilité élastique des plaques minces par la méthode des éléments finis. Université Laval. Faculté des Sciences. Département de Génie Civil. Section Mécanique des Glaces. Rapport GCS-81-08
- Frederking R, Gold L W 1975 Experimental study of edge loading of ice plates. *Canadian Geotechnical Journal* 12(4): 456-463
- Hirayama K, Schwarz J, Wu H C 1974 An investigation of ice forces on vertical structures. Iowa City, IA, University of Iowa. Iowa Institute of Hydraulic Research (IIHR Report 158)
- Kerr A D 1978 On the determination of horizontal forces a floating ice plate exerts on a structure. *Journal of Glaciology* 20(82): 123-134
- Kerr A D 1982 Remarks to the buckling analyses of floating ice sheets. In IAHR. International Association for Hydraulic Research. International symposium on ice, Québec, Canada, 1981. Proceedings Vol 2: 932-937
- Kheysin D Ye 1961 Opredeleniye vneshnikh nagruzok deystvuyushchikh na korpus sudna pri ledovom szhatii [Determination of external loads which act on the hull of a ship when under pressure from ice]. *Problemy Arktiki i Antarktiki* 7: 25-31
- KorzHAVIN K N 1962 Vozdeystviye l'da na inzhenernyye sooruzheniya. Novosibirsk, Akademiya Nauk SSSR. Sibirskoye Otdeleniye [English translation: Action of ice on engineering structures. CRREL Draft Translation 260, 1971]
- Michel B 1978 *Ice mechanics*. Québec, Presses de l'Université Laval
- Michel B 1981 Advances in ice mechanics. In POAC 81: the sixth International Conference on Port and Ocean Engineering under Arctic Conditions, Québec, Canada, 1981. Proceedings Vol 1: 189-204
- Michel B, Paradis M 1976 Analyse statistique des lois du fluage secondaire de la glace de rivière et de lac. Université Laval. Faculté des Sciences. Département de Génie Civil. Section Mécanique des Glaces. Rapport GCS-76-02
- Michel B, Toussaint N 1977 Mechanisms and theory of indentation of ice plates. *Journal of Glaciology* 19(81): 285-300
- Nevel D E 1980 Bending and buckling of a wedge in an elastic foundation. In Tryde P (ed) *International Union of Theoretical and Applied Mechanics. Physics and mechanics of ice. Symposium Copenhagen ...1979...* Berlin, etc, Springer-Verlag: 278-288
- Ralston T D 1978 Ice force design considerations for conical offshore structures. In POAC 77: the fourth International Conference on Port and Ocean Engineering under Arctic Conditions, St John's, Newfoundland, Canada, 1977. Proceedings Vol 2: 741-752
- Reinicke K M 1980 Analytical approach for the determination of ice forces using plasticity theory. In Tryde P (ed) *International Union of Theoretical and Applied Mechanics. Physics and mechanics of ice. Symposium Copenhagen...1979...* Berlin, etc, Springer-Verlag: 325-341
- Saeki H, Hamanaka K, Ozaki A 1978 Experimental study on ice force on a pile. In POAC 77: the fourth International Conference on Port and Ocean Engineering under Arctic Conditions, St John's, Newfoundland, Canada, 1977. Proceedings Vol 2: 695-706
- Sodhi D S, Hamza H E 1978 Buckling analysis of a semi-infinite ice sheet. In POAC 77: the fourth International Conference on Port and Ocean Engineering under Arctic Conditions, St John's, Newfoundland, Canada, 1977. Proceedings Vol 1: 593-604
- Tryde P 1973 Forces exerted on structures by ice floes. In 23rd International Navigation Congress, 1973. Section II. Subject 4. Brussels, General Secretariat of the Permanent International Association of Navigation Congresses: 31-44